26. The Measurement of Driver Describing Functions in Simulated Steering Control Tasks*

DAVID H. WEIR

Systems Technology, Inc.

AND

CHARLES K. WOJCIK

University of California

Measurements of driver describing functions in steering control tasks have been made using the Driving Simulator at UCLA. The simulator facility includes a **1965** Chevrolet sedan mounted on a chassis dynamometer, a moving model roadway and landscape, analog computation for the vehicle's handling dynamics, and a black and white TV camera-projector display system to provide the driver's visual display. The visual image was projected on a **6**×8 ft screen in front of the driver, giving a subtended horizontal angle of about **40".**

The task was to regulate against a random crosswind gust input on a straight roadway, in order **to** stay in the center of the lane. Five male drivers of varying age and driving experience were used in these exploratory studies. Although driving is a multiloop task in general, the forcing function and situation were configured *so* that an inner-loop visual cue feedback of heading angle **or** heading rate would dominate, and the driver's response was interpreted to be primarily single-loop. The driver describing functions were measured using an STI describing function analyzer. Three replications **for** each subject showed good repeatability within a subject. There were some intersubject differences as expected, but the crossover frequencies, effective time delays, and stability margins were generally consistent with the prior data and models for similar manual control tasks.

The results further confirm the feasibility of measuring human operator response properties in nominal control tasks with full (real-world) visual field displays, and they provide some verification and quantification of existing engineering models for the driver and the driver/vehicle system.

INTRODUCTION

Recent experimental studies using the UCLA driving simulator show the validity of simulator results relative to field studies, and provide an estimate of the driver's dynamic response in random input steering tasks. This paper describes the TV-projected model landscape driving simulator and presents experimental measures of driver-vehicle system response. Emphasis is placed on driver steering control of passenger vehicles on two-lane rural roads. Simulated tasks included overtaking and passing maneuvers and regulation against crosswind gusts. By mechanizing the vehicle's equations of motion on an analog computer, a broad range of vehicle handling can be simulated by adjusting the dynamic coefficients.

Simulation is useful in driving research because

- Limiting, critical situations can be studied safely.
- Controlled conditions can be created.

* This paper describes research results which are derived in part from work accomplished in cooperation with the California Business and Transportation Agency and **the U.S.** Department **of** Transportation, Bureau of Public Roads.

- Task variables can be changed systematically.

Typical practice (e.g., refs. **1** through **5)** generates the visual field image with

- Closed-circuit TV on scale models.
- Point light source shadowgram.
- Preprogrammed film.
- Computer generation of roadway abstraction.

The driver's station generally consists of a mockup of seat, controls, instrument panels, and windshield display. It is usually fixed-base, although simple moving-base devices have been used with limited success. Common deficiencies include

- Inadequate visual field size, framing, and reference points to indicate orientation of the driver or vehicle in the external world.
- The lack of realistic vehicle response as reflected in the movement of the displayed cues.
- Improper steering feel and deficient self-centering properties.

These deficiencies can be particularly troublesome in the study of steering control and vehicle handling tasks.

The newly developed simulator at UCLA tries to overcome some of these shortcomings. Its description comprises the next part of the paper. More details of its construction are given in reference **1.** In the remainder of the paper some exploratory describing function results are given for driver response with simulated random-appearing crosswind gust inputs.

SIMULATOR DESCRIPTION

The driver is seated in a **1965** Chevrolet sedan mounted on a chassis dynamometer facing the TV projection screen. A separate room contains the analog computer, **1**:72 scale model landscape, TV camera servo, and associated recording equipment. The setup is shown in figure **1.**

The functional block diagram is shown in figure **2.** The analog computer is an EAI TR–20. It contains the coupled lateral-directional equations of motion for the car which are summarized in appendix A, and provides heading rate and

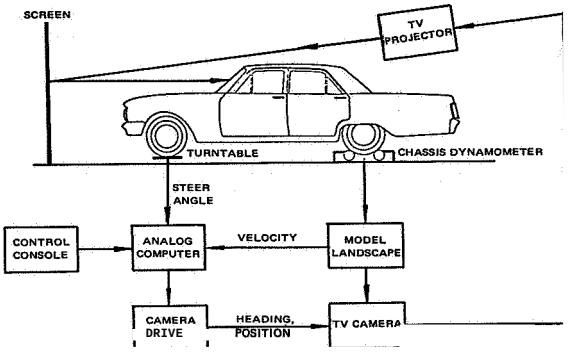

FIGURE 1.—Topological diagram of driving simulator.

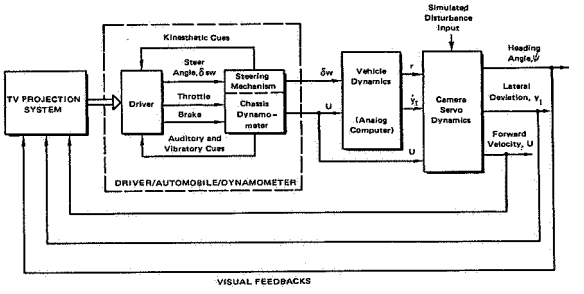

FIGURE 2.—Overall functional block diagram.

inertial lateral velocity signals to the two camera servos. Driver steering actions are fed to the analog computer, and the vehicle handling properties can be modified by changing the dynamic coefficients. Forward speed is controlled by the motion of the model landscape, slaved to the chassis dynamometer. The basic variables are shown in figure 2, using the notation of references **6** and 7. Table **1** summarizes this notation, the units commonly used, and the range of variables expected during simulator operation.

Although the simulator is fixed-base, the vibration of the rear wheels on the dynamometer provides tactile sensation which varies with speed. The car contains conventional power steering, with the front wheels mounted on spring-restrained swiveling turn tables to provide fairly realistic feel and self-centering properties. The self-centering properties are not perfect, however, and there is some hysteresis which the driver must remove to avoid drifts. The speedometer displays twice the actual rear wheel speed (the landscape belt speed is doubled accordingly) in order to keep road noise to a realistic level.

TABLE 1.—*Dejinition of Ximulation Variables*

Variable	Notation	Range
Forward velocity	U or U_0	0–100 ft/sec
Steer angle	δ_w	±0.2 rad
Heading angle	Ψ	±0.2 rad
Heading rate	r	±0.3 rad/sec
Lateral acceleration	a_y	±0.3 g
Lateral velocity	v	±10 ft/sec
Inertial lateral velocity	$\dot{y}_I$	±20 ft/sec
Lateral deviation	y_I	±20 ft

FIGURE 3.—Road scene as viewed by driver.

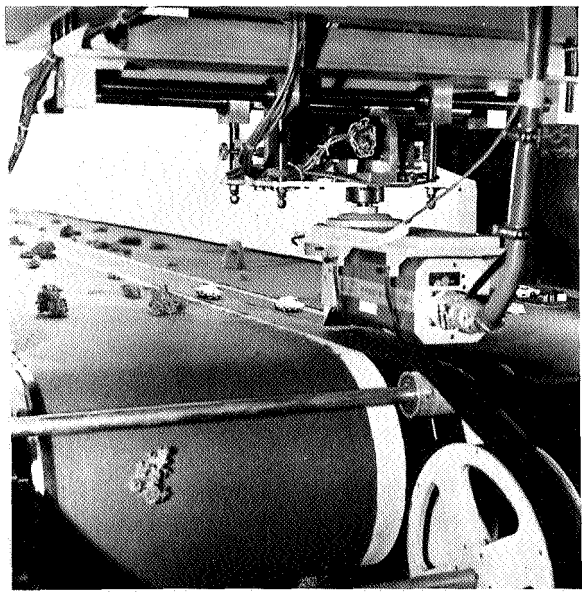

FIGURE 4.—TV camera, other vehicles, and model landscape.

This very approximately doubles the available acceleration rate at any given speed and gives a sensitive throttle response.

The TV camera is a black-and-white GPL Model 1000, with up to 1000 lines horizontal resolution, 15 H_z bandwidth, and a scan rate of 525 lines per frame. The camera lens is an f2.0 Schneider Xenon with 16 mm focal length, operating through two 1.5 in. silvered prisms to lower the optical axis to 0.75 in. (equivalent to a full-scale eye height of 48 in.). The TV projector is a Prizomatic 5XTP, mounted directly above the vehicle. It has a fixed orientation. The included horizontal angle of the visual field is about 40°, and the driver is seated relative to the projected image in correspondence to the camera image. The streamer and geometric cues used for directional control are strong and seem adequate for foveal and parafoveal vision. The resolution of the projected image is such that an object the size of an oncoming vehicle can be distinguished as present (if not identified) at an equivalent full-scale distance of about one quarter mile (the length of the moving belt landscape). The overall impression is one of driving in desert terrain under a heavy, dark overcast. After familiarization, the subjects reported that it seemed very realistic. A typical projected scene as viewed by the driver is shown in figure 3.

Provision is also made to control and measure the position of lead and oncoming cars relative to the subject vehicle. These other vehicles are fixed to tapes (roadway lanes) which move relative to the model landscape. This is shown in figure 4, together with the TV camera mount.

The lack of motion cues always has at least a minor effect on a fixed-base simulation of this type. In driving maneuvers and disturbance regulation the lateral acceleration motion cue provides a useful high frequency (rapid) cue which alerts the driver to an input onset, as well as providing feedback regarding the initial results of his steering response. Without vestibular cues the driver must wait until the change in the visual display exceeds threshold, and this delay is increased by any camera servo deadband. The net effect can be treated as an increase in the driver's effective time delay, and this results in reduced performance potential. In this simulation the effect does not appear to be significant. This is confirmed by the experimental results (ref. 1), which show good comparison between field and simulator results for the same tasks and subjects.

SIMULATED VEHICLE DYNAMIC RESPONSE

Several vehicles with different handling properties have been simulated to date. The one used in the experiments reported here was a nominally loaded full-size station wagon with less than ideal handling properties.

The assumed design parameters and vehicle stability derivatives are given in table *2*, using the notation of the appendix to this paper. Substituting these stability derivatives into the lateral-directional equations of motion and rearranging, gives the following vehicle motion to steer angle input transfer functions.

Lateral velocity:

$$\frac{v}{\delta_w} = \frac{91(s-16.4)}{[s^2+2(.79)(3.3)s+(3.3)^2]} \qquad (1)$$

Heading rate:

$$\frac{r}{\delta_w} = \frac{19.5(s+2.8)}{[s^2+2(.79)(3.3)s+(3.3)^2]} \qquad (2)$$

Lateral deviation (position in lane):

$$\frac{y_I}{\delta_w} = \frac{91[s^2+2(.19)(7.4)s+(7.4)^2]}{s^2[s^2+2(.79)(3.3)s+(3.3)^2]}. \qquad (3)$$

The dynamic response properties are similar to those of the test vehicle used in prior field experiments (ref. 8).

The analog computer diagram is shown in figure **5**. The kinematic variation of speed in the equations (i.e., the $U\psi$ term) was accounted for by using the speed sensed by a belt-driven tach-generator. Some of the stability derivatives Y_v, Y_r, N_v, and N_r are inversely proportional to speed in the nominal driving range (**45** to **60** mph), however, fixed settings corresponding to **60** mph were used for simplicity. Where possible, the experimental tasks were planned for a constant **60** mph. Operation at speeds below the design values results in a less responsive vehicle than would normally be the case if the derivatives were speed varying (see ref. **6).**

TABLE 2.—*Dynamic Parameters for Simulated Car*

Design parameters		Stability derivatives	
m, slugs	151	Y_v, sec^{-1}	−2.8
U_0, ft/sec	88	Y_r, ft/sec-rad	1.33
Y_{α_1}, lb/rad	6860	N_v, rad/ft-sec	.05
Y_{α_2}, lb/rad	11700	N_r, sec^{-1}	−2.45
a, ft	5.77	Y_{δ_w}, ft/sec^2-rad	91
b, ft	4.14	N_{δ_w}, sec^{-2}	19.5
I_z, slug-ft^2	4060	N_v, rad/ft-sec	−,003
ℓ, ft	9.91	Y_v, sec^{-1}	−,035

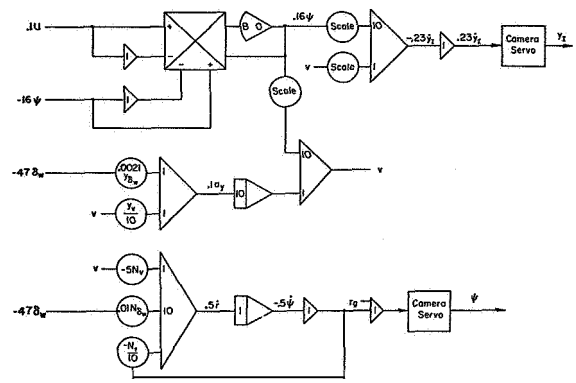

FIGURE 5.—Analog computer mechanization.

Although the analog computer provides a good representation of the vehicle's steering response, the camera servo drive for heading has a small amount of backlash which results in a deadband and hysteresis. The magnitude of the deadband is less than a degree, but it may be important for small heading corrections and accurate disturbance error regulation.

OVERTAKING AND PASSING EXPERIMENTS

A major objective of the overall research study was to replicate full-scale field measurements of driver control for simulator validation. Previously published response and performance measurements for overtaking and passing tasks with and without an oncoming vehicle (ref. 8) provided a useful field data base. These tasks were repeated in the simulator using the same driver subjects so that at least some subjects served as their own control. If transfer effects are negligible, for these subjects any differences would be due to physical effects such as lack of vestibular cues, degree of visual realism, and differences in handling dynamics.

Details of these experiments are given in reference **1.** To summarize, the simulator results

were in good agreement with the previously published field data (ref. **6)** for comparable tasks. The same relative changes occurred in field and simulator as the tasks changed. With comparable controlled element dynamics and the same driver subject, both the absolute levels of driver/vehicle response in a given task and the magnitudes of the change between situationswere quite similar in field and simulator. These results confirmed the validity of the simulator task with respect to evoked response and performance for nominal steering tasks.

RANDOM CROSSWIND GUST EXPERIMENTS

In contrast to overtaking and passing, continuous closed-loop operation by the driver dominates in the presence of a random-appearing disturbance input such as a crosswind gust. With continuous control, on-the-average frequency response properties of the driver can be measured as a describing function.

Models for the driver in continuous control task have been described previously (e.g., refs. **7** and **9).** Several feedbacks such as heading angle or rate, and path angle or rate, were shown to be good "inner-loop" control cues; while a necessary "outer loop" for trim control seems to be lateral deviation in the lane. With a dynamic simulator of the sort used in the experiments it is possible to structure regulation tasks and measure the driver's response under the interpretation that certain feedbacks are dominant; and this is accomplished below. Investigation of the more fundamental question of which feedback structures are operant in a given driving situation requires extension of these experimental techniques, and has yet to be accomplished.

These experiments were set up so that the driver's steering response resulted from his operation on heading angle, ψ, and lateral deviation y_I cues. The multiloop block diagram for this case is the simplified version of figure 2, as shown in figure **6.** The driver's task is to maintain the car in the center of the lane (at **60** mph) in the presence of the equivalent crosswind gust signal.

Because only one gust input is being used, the analyses concentrated on the middle and high frequency driver response data which are dominated by the heading disturbance in this task. Then the lateral deviation outer loop is assumed to result in low frequency corrections to reduce errors which accumulate despite the driver attempting to maintain the car's heading parallel with the roadway. The fidelity of the measurements is reflected in the linear correlation in the data between the disturbance input and the driver's steering response, as measured by $\bar{\rho}_e^2$.

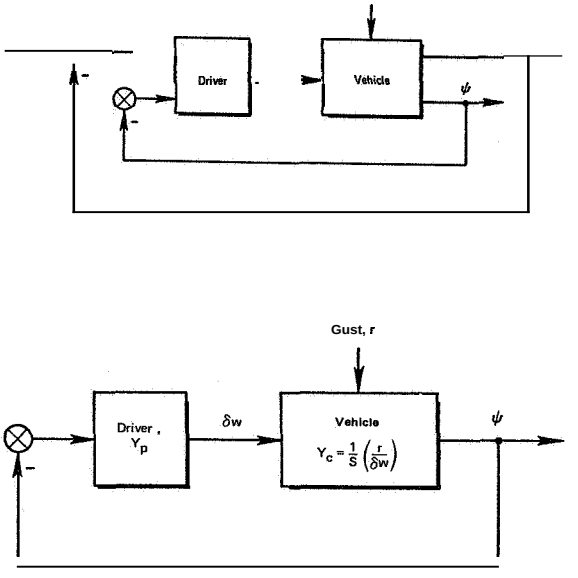

FIGURE 7.—Simplified system for data interpretation.

With this interpretation, the driver/vehicle system takes the single-loop form of figure **7,** which accounts for its dominant characteristics in this task. The vehicle's dynamics Y_c are given by integrating the heading rate to steer angle transfer function in equation (2); and the result is approximately a simple integration or K/s controlled element; i.e.,

$$Y_c = \frac{\psi}{\delta_w} = \frac{1}{s}\left(\frac{r}{\delta_w}\right) \doteq \frac{K_c}{s}. \tag{4}$$

In this case the driver model Y_p takes the form of a pure-gain-plus-time-delay,

$$Y_p = \frac{\delta_w}{\psi_e} = K_p e^{-\tau_e j\omega} \tag{5}$$

as shown in references **7** and **9.** The complex frequency $j\omega$ is used (instead of s) in the driver

describing function because the describing function is computed by taking the ratio of cross spectra which are Fourier transforms.

The heading rate gust disturbance signal r_g was a random-appearing sum of equal amplitude sine waves with component frequencies at 0.5, **1.26, 3.0,** and **6.3** rad/sec, and an rms amplitude **of 1.8** deg/sec. The camera servo acted as an integrator which produced a heading angle disturbance that rolled off at **20** dB/decade, **as** if low pass filtered. The resulting heading angle disturbance appeared to have a bandwidth of about **0.7** to **1.0** rad/sec on the display, with an rms amplitude of approximately **1.7°.** The subjective effect is not unlike that of driving a very gust–sensitive car in an intermittent crosswind.

DRIVER DESCRIBING FUNCTION DATA

The driver model (ref. **7)** provides for his equalization of the vehicle dynamics such that the combined driver/vehicle system properties are approximately invariant. The result is that the driver/vehicle describing function for closed-loop operation on a displayed cue has the general form:

$$\frac{\psi}{\psi_e} = Y_p Y_c \doteq \frac{\omega_c}{j\omega} e^{-(\tau_e j\omega + \alpha/j\omega)} \tag{6}$$

where Y_p is the driver and Y_c is the controlled element. The parameter ω_c is the Bode crossover frequency (or closed-loop system gain) and provides a good estimate of the driver/vehicle system bandwidth. The effective time delay is τ_e as shown in equation (5). The additional parameter α accounts for the driver's low frequency phase lag (often attributed to his neuromuscular properties) which is sometimes observed.

The output-to-error describing function of equation **(6)** was measured directly, on-line, using a Systems Technology, Inc., Describing Function Analyzer (DFA), Model **1001.** This DFA also supplies the random-appearing heading rate disturbance input described above. The driver describing function Y_p is computed from ψ/ψ_e by dividing by the assumed vehicle dynamics or controlled element, $Y_c = \psi/\delta_w$. Each experimental run lasted **100** sec.

Estimates of driver/vehicle model parameters given in equation **(6)** have been made using the DFA results for several runs on each **of** five driver subjects whose backgrounds are given in

TABLE 3.—*Subject Background*

Subject	Age	Years driving	Personal vehicle	Passes on rural roads in last: Month	Passes on rural roads in last: Year	Remarks on simulator realism
B	**48**	**18**	Mercury Comet **(1962)**	**0**	**10**	.....
C	**23**	**7**	Ford Econoline Van **(1969)**	...	...	Steering oversensitive. Simulation seemed OK for cues.
D	**34**	**18**	Ford Mustang **(1965);** VW squareback **(1969)**	**15**	**50**	Vehicle response realistic. Easy to project oneself into task ***so*** that lack **of** visual field acuity and limited peripheral cues are not noticed. Lateral acceleration cues are missed in first fraction of second following steering inputs.
E	**30**	**14**	Volvo **144 (1968)**	0	**20**	Visual scene like heavy overcast with light rain. Some ill effects due to lack **of** motion cues. Vehicle seemed somewhat oversensitive and gusts were too lively. Considering limitations, however, simulator seemed surprisingly realistic.
F	**30**	**13**	Buick station wagon **(1964);** Karman Ghia **(1968)**	**10**	**30**	Couldn't judge center **of** lane well. Vehicle handled naturally. Visual scene was like light snow condition.

table **3.** The individual data runs are shown in figure 8(a) through (e), with Y_pY_c on the right and the computed Y_p on the left. The averaged parameters for the fitted Y_pY_c curves are summarized in table **4.** Also shown in table **4** are the closed-loop phase margin φ_m, gain margin G_M, and zero phase margin crossover frequency, ω_u, which relate to system stability and the quality of control. The average linear correlation, ρ_e^2, is the fraction of the total heading rate error which is linearly correlated with the gust input—the average coherence. Values in the range of 0.5 to **0.6** indicate that the majority of the driver's steering actions are heading angle or heading rate corrections that are correlated with the gust input, and these values are consistent with comparable instrument panel data. σ_e^2/σ_i^2 is the heading rate error variance over the heading rate input r_g variance, and the larger values in figure 8 may imply that the driver is using a low frequency heading bias to correct residual errors in lateral deviation (see fig. **6).**

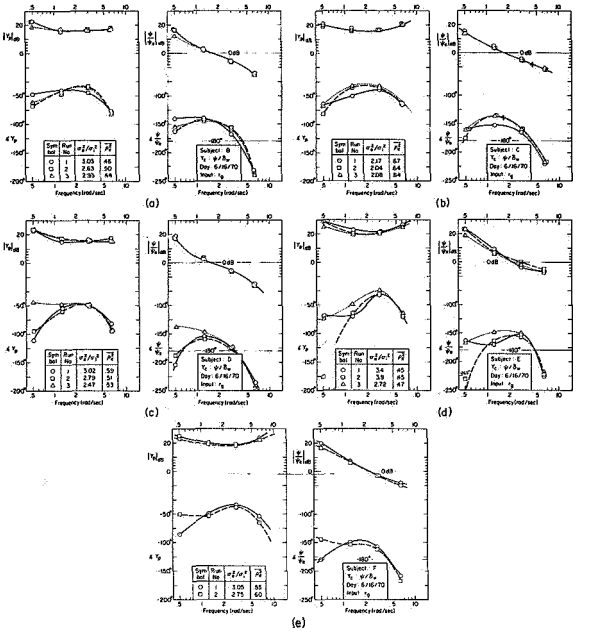

FIGURE 8.—Describing function data.

The dominant features of the data are the consistent similarity in crossover frequency, effective time delay, and stability margins. This is not only true within one subject (as expected), but over all subjects. The crossover frequency is bounded on the low side by the gust bandwidth—the former has to be nearly twice the latter to achieve effective control (e.g., ref. 9). Crossover frequency is limited on the upper side by the effective time delay (due to driver and car) and stability considerations. The repeatability in the data is associated with these task-related constraints.

The measured driver response properties and stability margins are compatible with inner-loop crossover frequency predictions made for similar vehicle/task situations in prior studies (e.g., refs. **7** and **S),** suggesting that heading angle is a reasonable inner-loop cue in the multiloop driver/vehicle system structure. Note that lagged heading rate is a reasonable alternative, but simple proportional operation on (unlagged) heading rate is not a compatible alternative because **(1)** it is inconsistent with the previously noted form of Y_pY_c based on a large body of prior data, and **(2)** the effective gust bandwidth of **6.3** rad/sec would then be prohibitively large. Finally, the observed values of τ_e and φ_m are more consistent with prior data for $Y_c=K/s$ (i.e., heading angle) than for $Y_c=K$ (i.e., heading rate).

The "peaking up" of the high frequency amplitude ratio for subjects C, E, and F, in figure 8(b), (d), and (e), indicate that they are using lead equalization to offset the additional high frequency lag in the simulated car. The result is

TABLE 4.—*Summary of Describing Function Results*

Subject	ω_c, rad/sec	φ_m, deg	G_m, dB	τ_e, sec	ω_u, rad/sec	ρ_E^2
B	**1.7**	**35**	**8.3**	**0.34**	**3.8**	**0.47**
C	**1.8**	**36**	**7.5**	**.35**	**4.1**	**.65**
D	**1.7**	**24**	**6.9**	**.41**	**3.3**	**.54**
E	**2.9**	**27**	**2.9**	**.24**	**4.3**	**.46**
F	**2.3**	**28**	**5.6**	**.32**	**4.3**	**.58**

reflected in table 4 as a lower effective time delay which in turn permits a higher crossover frequency (with the same stability margins) and better gust regulation performance. The stability margins for each driver are large enough to give smooth (comfortable) response, as well as rapid error reduction. The α measures are somewhat unreliable because they represent a least square fit to only the middle two frequency points.

These exploratory data show that repeatable measures of driver response in closed-loop steering control tasks can be made. Not unexpectedly, the results are consistent with predictions from prior (empirically derived) driver/vehicle models, and they provide added insight into the multiloop feedback structure the human operator may adopt when provided with a cue-rich, real-world visual field.

CONCLUSIONS AND IMPLICATIONS

A major objective was to implement and exercise a driving simulator useful in the study of driver control processes, and to establish the validity of simulation results by comparison with published field data for similar subjects and tasks. This has been accomplished. The dynamic response and performance of the simulator are subjectively realistic, and it yields data which are similar to field data. It also shows the same sensitivity to variations in tasks and conditions as the field data. By mechanizing the vehicle's differential equations on an analog computer, a broad range of vehicles can be simulated by simply adjusting dynamic coefficients.

Driver describing functions have been measured in a simulated crosswind gust regulation task. These exploratory results were repeatable and compatible with existing driver/vehicle system models. The numerical parameters confirmed prior estimates of closed-loop properties and provided new insight to the possible driver/vehicle system multiloop structure.

ACKNOWLEDGMENTS

The authors wish to thank Richard Klein and R. Wade Allen of Systems Technology, Inc., for their assistance in simulating the vehicle dynamics and accomplishing the driver describing function measurements; and Richard Maynard of the Institute of Transportation and Traffic Engineering, UCLA, for his part in operating and maintaining the simulation system.

REFERENCES

1. WOJCIK, C. H.; AND WEIR, D. H.: Studies of the Driver as a Control Element, Phase No. 2. Rept. 70–73, UCLA Inst. of Transportation and Traffic Engineering, July 1970.
2. ANON.: Proceedings of a Conference on Mathematical Models and Simulation of Automobile Driving. Mass. Instit. of Tech. Sept. 28–29, 1967.
3. HULBERT, SLADE: Survey and Comparisons of Simulation Techniques for Automobile Driving Research. Paper No. 69–WA/BHF–11, ASME, Nov. 1969.
4. ANON.: Proceedings of General Motors Corporation Automotive Safety Seminar, No. 24. July 11–12, 1968.
5. SUNAGA, KAZUO; IIDA, SHIN; AND FUJIOKA, SHIZUO: A Driving Simulator for Stability of a Motor Vehicle. Stability and Control Committee, Society of Automotive Engineers of Japan, Inc., Oct.–Nov. 1969.
6. WEIR, D. H.; SHORTWELL, C. P.; AND JOHNSON, W. A.: Dynamics of the Automobile Related to Driver Control. Tech. Rept. 157–1, Systems Technology, Inc., July 1966 (also SAE Paper 680194).
7. WEIR, DAVID H.; AND MCRUER, DUANE T.: A Theory for Driver Steering Control of Motor Vehicles. Highway Research Record No. 247, 1968.
8. WEIR, DAVID H.; ALEX, FREDERIC R.; AND RINGLAND, ROBERT F.: Driver Control During Overtaking and Passing Under Adverse Conditions. Tech. Rept. 174–1, Systems Technology, Inc., May 1969.
9. MCRUER, D.; AND WEIR, D. H.: Theory of Manual Vehicular Control. Ergonomics, vol. 12, no. 4, 1969, pp. 599–633.

APPENDIX

Lateral-Directional Vehicle Dynamics

The lateral motions of a car which dominate in steering control and are represented in the simulator system are shown in figure **A–1.** The symbols are defined in table **1.**

The lateral-directional matrix equation for a car with lateral velocity v and heading rate r degrees of freedom are derived in reference **6** and summarized below:

$$\begin{bmatrix} s-Y_v & U_0-Y_r \\ -N_v & s-N_r \end{bmatrix}\begin{bmatrix} v \\ r \end{bmatrix}=\begin{bmatrix} Y_{\delta_w} \\ N_{\delta_w} \end{bmatrix}\delta_w+\begin{bmatrix} Y_{v_g} \\ N_{v_g} \end{bmatrix}v_g \qquad \text{(A–1)}$$

s is the Laplace Transform complex variable. The front wheel steer angle is δ_w and v_g is a lateral velocity gust. The stability derivatives are defined in terms of vehicle and tire design parameters by the following expressions:

$$Y_v=\frac{-2}{mU_0}(Y_{\alpha_1}+Y_{\alpha_2})$$

$$Y_r=\frac{2}{mU_0}(bY_{\alpha_2}-aY_{\alpha_1})$$

$$N_v=\frac{2}{I_{zz}U_0}(b\,Y_{\alpha_2}-aY_{\alpha_1})$$

$$N_r=\frac{-2}{I_{zz}U_0}(a^{2}Y_{\alpha_1}+b^2Y_{\alpha_2})$$

$$Y_{\delta_w}=\frac{2}{m}Y_{\alpha_1}$$

$$N_{\delta_w}=\frac{2a}{I_{zz}}Y_{\alpha_1}$$

$$Y_{v_g}=\frac{qA}{mU_0}C_{y_{\beta_g}}$$

$$N_{v_g}=\frac{qA\ell}{I_{zz}U_0}C_{n_{\beta_g}}.$$

The design parameters on the right of these equations are as follows

- m is the total vehicle mass
- U_0 is the nominal forward velocity
- Y_{α_1} is the side force due to front tire slip angle
- Y_{α_2} is the side force due to rear tire slip angle
- a is the distance of the c.g. aft of the front axle
- b is the distance of the c.g. aft of the rear axle
- I_{zz} is the total vehicle yaw moment of inertia

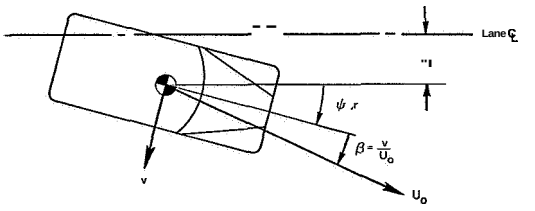

FIGURE A-1.—Motion quantities for directional control.

q is the aerodynamic pressure
A is the projected frontal area
$\ell = a + b$ is the wheel base
$C_{y_{\beta_0}}$ and $C_{n_{\beta_0}}$ are the aerodynamic coefficients.

More detailed descriptions are given in reference 6.

Normally $|Y_r|$ is much less than U_0. Another simplification shown in equation (A–1) is the deletion of the gust terms (Y_{v_g} and N_{v_g}) from the left-hand side because they are small relative to the tire forces and moments (Y_v and N_v) at reasonable speeds. They are included on the right side to provide for force and moment disturbance inputs to the simulation.

These two-degree-of-freedom equations do not include the roll mode. It can have considerable influence on them by modifying the effective Y_{α_1} and Y_{α_2}, mainly due to roll steer and camber thrust effects. Knowledge of the complete three-degree-of-freedomequations and data allows this correction to be made in the two-degree-of-freedom model. Another result of including a roll degree of freedom is the appearance of a usually inconsequential high frequency dipole pair in the lateral-directional transfer functions. Hence, the two-degree-of-freedom equations used in the simulation reflect the major effects of the roll without including it explicitly.